LASER INTERFEROMETER GRAVITATIONAL WAVE OBSERVATORY
- LIGO -
CALIFORNIA INSTITUTE OF TECHNOLOGY
MASSACHUSETTS INSTITUTE OF TECHNOLOGY

Document Type	**LIGO-T980027-01 - D**	9/4/98

Baffling Requirements for the 4K and 2K IFO

Michael Smith

Distribution of this draft:

This is an internal working note
of the LIGO Project.

California Institute of Technology
LIGO Project - MS 51-33
Pasadena CA 91125
Phone (626) 395-2129
Fax (626) 304-9834
E-mail: info@ligo.caltech.edu

Massachusetts Institute of Technology
LIGO Project - MS 20B-145
Cambridge, MA 01239
Phone (617) 253-4824
Fax (617) 253-7014
E-mail: info@ligo.mit.edu

WWW: http://www.ligo.caltech.edu/

LIGO-DRAFT

1 INTRODUCTION

This paper will discuss the need to provide baffles at various locations within the 2K and 4K LIGO interferometers, and will provide supporting calculations to justify the conclusions. The requirements for baffling within the IFO have been determined based on the criteria that direct glints and scattering from surfaces will not exceed the initial LIGO scattered light requirement, as defined in the LIGO SRD, LIGO_E950018-02-E, and as detailed in COS DRD LIGO-T970071-02-D.

2 SCATTERING FROM COC SURFACES

The need for baffles within the beam tube region and at the ends of the tube is dependent upon the scattering characteristics of the COC mirrors. The scattering probability per solid angle (BRDF) of the superpolished COC optical surfaces can be described empirically by a fractal expression with coefficients chosen to match the experimental data.

$$BRDF(\theta) = \frac{BRDF_0}{(1 + b\theta^2)^{\frac{c+1}{2}}}$$

Scattering data from two representative samples of superpolished fused silica mirror surfaces was obtained from the Pathfinder Optics. GO S/N 5 represents the lowest observed surface microroughness, and CSIRO S/N 2 is assumed to be typical of the LIGO superpolished mirrors. A fit of the one-dimensional surface roughness power spectral density data to the fractal expression was done by A. Lazzarini[1] for both these optical surfaces. The resulting BRDF is shown in figure 1.

GO S/N 5 $$BRDF_2(\theta) = \frac{1000}{(1 + 5.302\times10^8 \cdot \theta^2)^{1.55}}\ \mathrm{sr}^{-1}$$

CSIRO S/N/ 2 $$BRDF_1(\theta) = \frac{2755}{(1 + 8.508\times10^8 \cdot \theta^2)^{1.24}}\ \mathrm{sr}^{-1}$$

A significant amount of small angle scattered light from the COC mirrors will pass out the far end of the beam tube. This is calculated by integrating the BRDF of the COC mirror over the solid angle subtended by the far end of the beam tube.

$$P_2(\theta_{max}) := P_i \cdot 2\cdot\pi \cdot \int_0^{\theta_{max}} BRDF_2(\theta)\cdot\sin(\theta)\,d\theta$$

The calculation was made for the two representative BRDF functions described above, with 5000 watts in the arm cavity incident on the mirror. The results are shown in figure 2

LIGO-DRAFT

1. Scattered Light and its Control in the LIGO Beam Tubes, Albert Lazzarini, LIGO Science Meeting Talk, 4/1/97

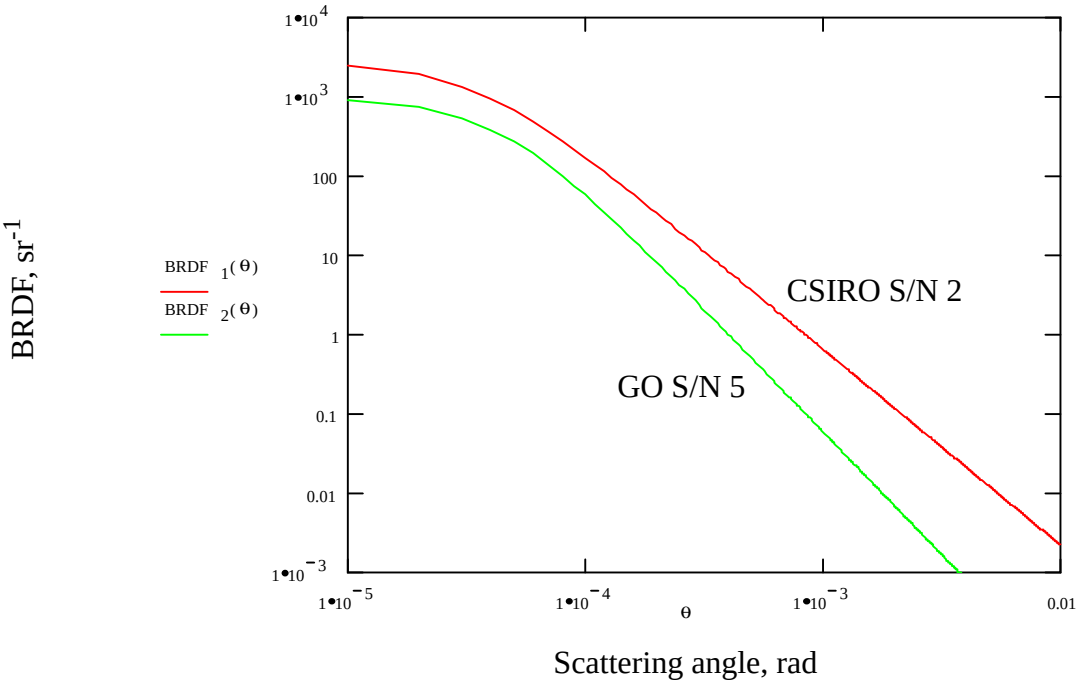

Figure 1: BRDF of Pathfinder Optics: GO S/N 5 and CSIRO S/N2

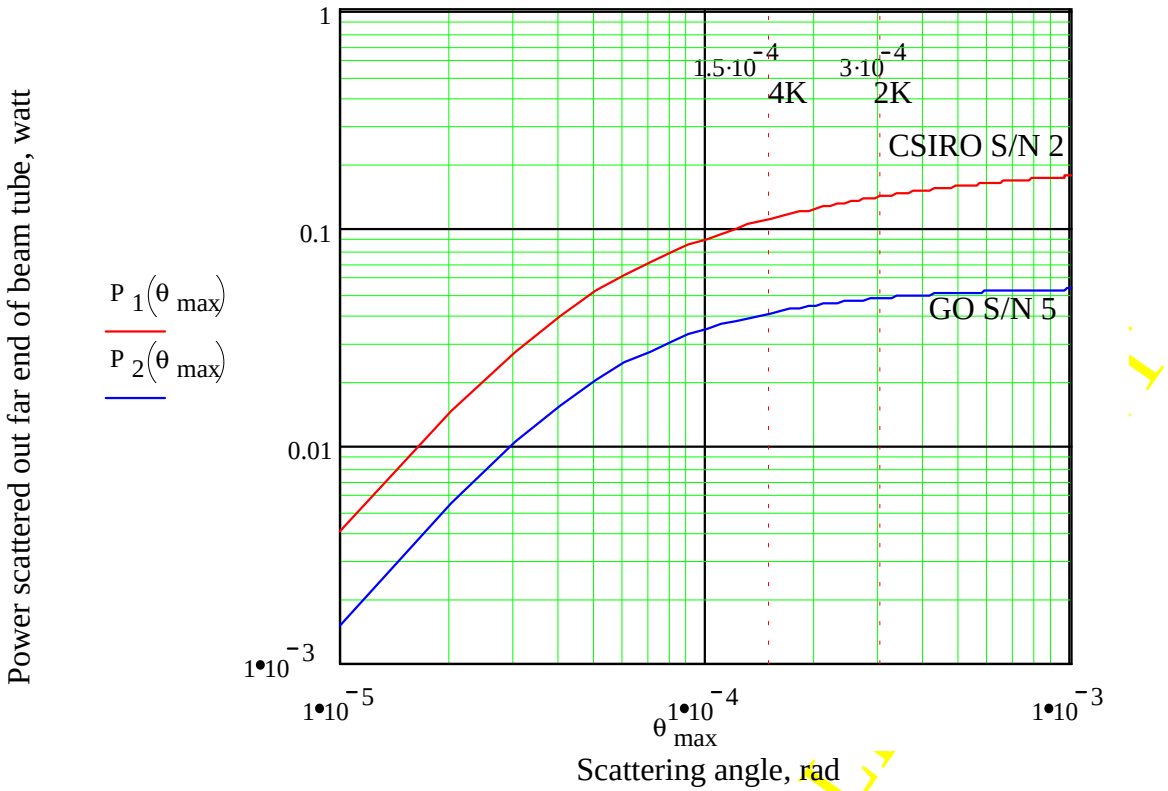

Figure 2: Scattered power from COC mirror out the far end of the beam tube

The scattering angles subtended by the far end of the 2K and 4K beam tubes are shown for reference.

scattering angle subtended by the far end of the 2K beam tube 3×10^{-4} rad

scattering angle subtended by the far end of the 4K beam tube 1.5×10^{-4} rad

Note that with the larger BRDF optic, approximately 150 miliwatts will be scattered out the far end of the beam tube in the 2K IFO.

3 STRAY LIGHT BAFFLES

3.1. Baffling of the ITM and the ETM Mirrors in the Arm Cavity

The baffle shown schematically in figure 3 is designed to block the ETM diffusely scattered light from hitting the surfaces of the BSC vacuum housing, backscattering onto the ETM, then scattering again from the ETM into the IFO. The stray light baffle will attenuate the scattered light as a result of the relatively small BRDF of the baffle surface. The specularly reflected light from the baffle will be redirected toward the beam tube walls at a large enough angle so that the probability of scattering back into the IFO will be relatively small. In exactly the same manner, the diffusely scattered light from the ITM will be blocked, as shown in figure 4.

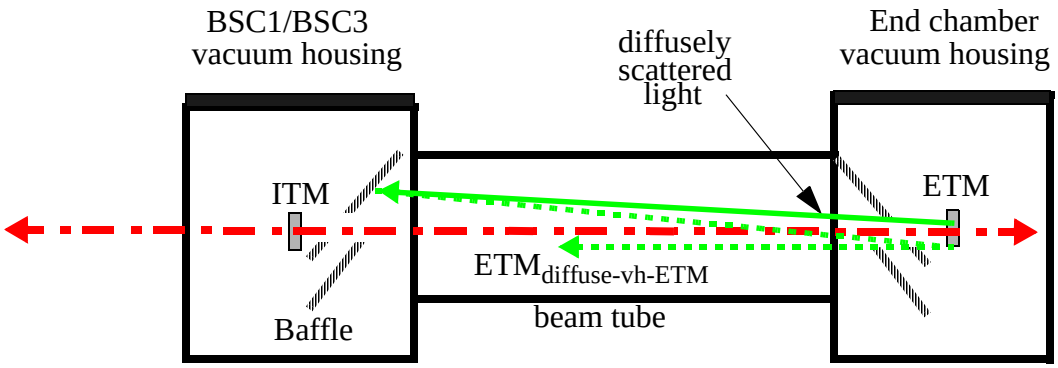

Figure 3: Diffuse Scattering from ETM, backscattered from the BSC Vacuum Housing, and re-scattered by ETM into the IFO

LIGO-DRAFT

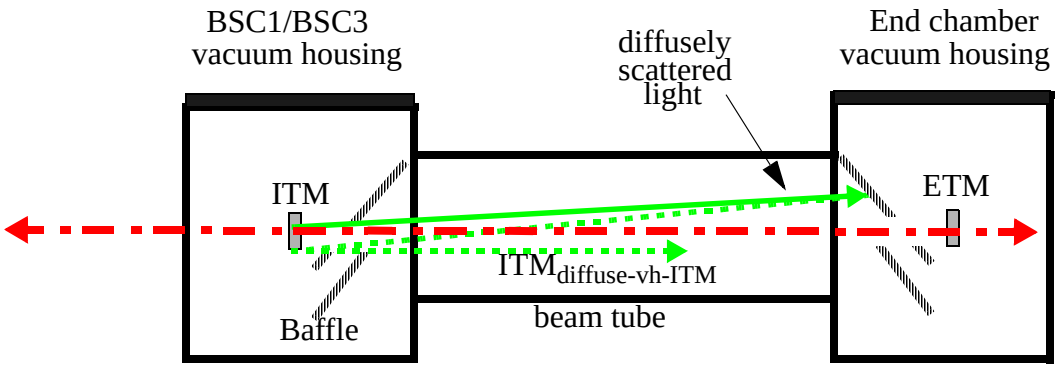

Figure 4: Diffuse Scattering from ITM, then Backscattered from the End Vacuum Housing, and Re-scattered by ITM into the IFO

3.1.1. Large-angle Scattering from the ITM and ETM, Scattering Calculations

The diffusely scattered light P_{diff} from the COC passing out the ends the beam tube may hit the chamber walls and cause a glint back into the IFO beam. The glint would exceed the scattering noise requirement as shown in Table 1 on page 6. However, the glint will be blocked by the COC baffles. The scattered light from the COC baffles meets the LIGO scattering requirement.

The glint power can be estimated as follows (See "Ghost Beam Glint Calculations" on page 20.).

$$P_g = P_{diff} \cdot \frac{2R\lambda}{\pi^2 w^2} \eta_{glint} .$$

Some of the light hitting the baffle will be backscattered to the original ITM or ETM source surface and then re-scatter back into the IFO. The power scattered into the IFO is given by the following

$$P_s = P_{diff} \cdot BRDF_{baff} \cdot \frac{A_{COC}}{L^2} \cdot BRDF_{COC} \cdot \Delta\Omega$$

The light power back-scattered from the COC baffles into the IFO was calculated using the following values:

BRDF of baffle	$BRDF_{baff} = 1\times10^{-3}$ sr^{-1}
area of COC scattering surface	$A_{COC} = \pi r^2 = 4.9\times10^{-2}$ m^2
separation between 4K COC and baffle	L=4000 m
separation between 2K COC and baffle	L=2000 m
BRDF of COC at 3.0×10^{-5} rad incidence angle	$BRDF_{COC}(3\times10^{-5} rad) = 1\times10^{3}$ sr^{-1}
scattering acceptance cone	$\Delta\Omega = 2.7\times10^{-10}$ sr.

The results are shown in Table 1 on page 6.

LIGO-DRAFT

Table 1: Summary of Scattering from COC in Arm Cavity Out the End of the Beam Tube

Parameter	*4K*	*2K*
scattered power out the beam tube, watt	0.110	0.140
radius of chamber wall, m	1.5	1.5
ITM beam parameter, w, mm	36.3	26.9
ETM beam parameter, w, mm	45.7	31.5
ITM glint power from chamber wall, watt	2.7×10^{-13}	4.9×10^{-13}
ETM glint power from chamber wall, watt	1.7×10^{-13}	3.6×10^{-13}
scattered power from COC baffle, watt	9.1×10^{-20}	4.6×10^{-19}
scattered light requirement, watt	3.2×10^{-18}	3.2×10^{-18}

3.1.2. Edge Diffraction from Aperture in the COC Baffle

The diffracted power into the IFO from the 124 mm radius aperture ITM COC baffle tilted 33 deg from the beam axis is 2.0×10^{-24} watts. Similarly, the power diffracted into the IFO from the tilted ETM COC baffle with a 124 mm radius aperture is 6.4×10^{-21} watts. See “Edge diffraction” on page 24. This *does not exceed* the scattered light power requirement for diffuse light in the arm cavity $< 3\times10^{-18}$, (see COS DRD LIGO-T970071-02-D).

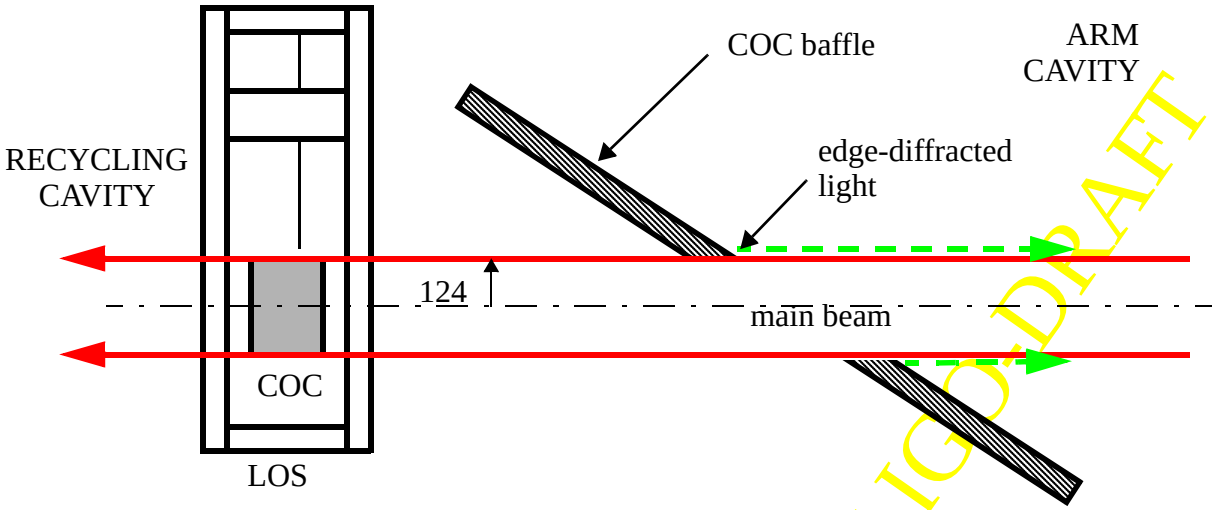

Figure 5: Edge diffraction by COC baffle

LIGO-DRAFT

3.2. Are Baffles Needed in the Vacuum Manifold?

The following discussion will show that 1) *baffles are not needed in the vacuum manifold* segments at both ends of the beam tubes, 2) *baffles are needed at the near side of the cryopumps.*

3.2.1. 2K IFO Vacuum Manifold Scattering Geometry

The light scattered at small-angles from the surface of the 2K ITM mirror (shown in green) toward the beam tube will backscatter from the bare walls of the vacuum manifold, then re-scatter from the surface of the 2K ITM into the IFO. The predominant scattering surfaces as shown in figure 6 are the walls of the following vacuum manifold sections: B-8A, B-1A, BE-5A, B-9A, A-1A, the cryopump liner surfaces of CP2, BE-4A, the beam tube, BE-4C, the cryopump liner surfaces of CP5, and A-1C. Only light scattered from the vacuum manifold surfaces in the 2 km length section of the beam tube out to the mid station need be considered, because scattered light from surfaces beyond the mid-section will be blocked by the stray-light baffle in front of the 2K ETM and will not scatter into the 2K ITM.

The light scattered from the 2K ETM mirror will backscatter from the same walls of the vacuum manifold described above, except in reverse order; and will then re-scatter from the surface of the ETM into the IFO.

In addition, light scattered from the surface of the 4K ITM mirror on BSC-3 toward the beam tube, as shown in figure 7, will pass through the 4K beam hole in the baffle at BSC-7 and will scatter from the same surfaces of the vacuum manifold described above in the near 2km section of the IFO

.

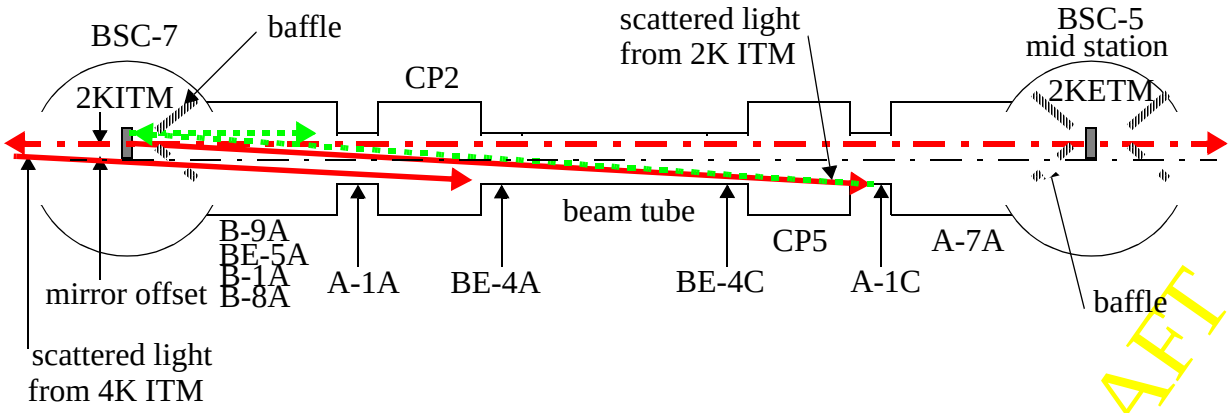

Figure 6: 2K IFO, scattered light from ITM, backscattering from vacuum manifold walls (shown in green) then re-scattering from ITM into the IFO.

3.2.2. 4K IFO Vacuum Manifold Scattering Geometry

The light scattered from the surface of the 4K ETM toward the beam tube (shown in green) will backscatter from the bare walls of the vacuum manifold, then re-scatter from the surface of the 4K ETM into the IFO, as shown in figure 7. The scattering surfaces are the walls of the following

LIGO-DRAFT

vacuum manifold sections: A-7C, A-1E, the cryopump liner surfaces of CP8, BE-4G, the beam tube, BE-4E, the cryopump liner surfaces of CP6, and A-14A.

In addition, a portion of the 4K ITM scattered light will also pass through the 4K beam holes in the mid station baffles on BSC-5 and will be intercepted by the 4K ETM baffle.

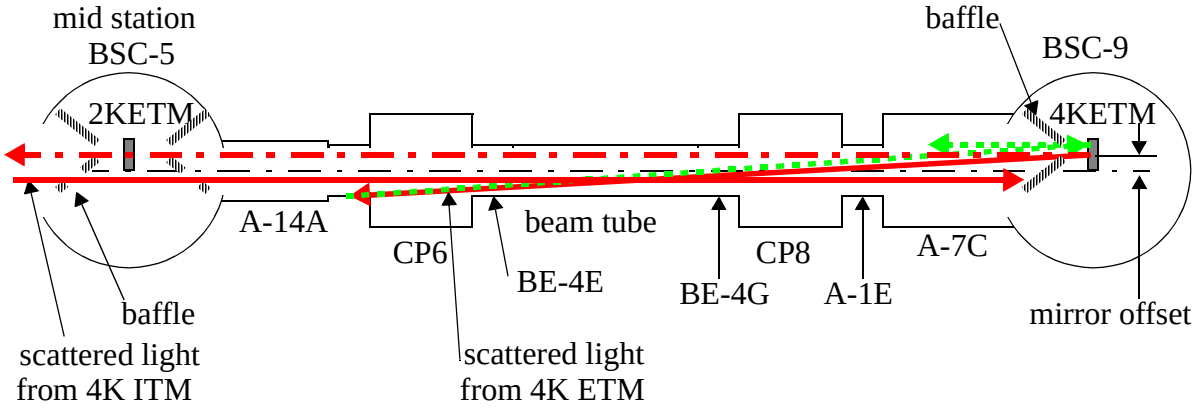

Figure 7: 4K IFO, scattered light from ETM, backscattering from vacuum manifold walls (shown in green) then re-scattering from ETM into the IFO.

3.2.3. Vacuum Manifold Light Scattering Calculations

The micro-roughness of the COC surface determines the large angle scattering characteristics of the COC. In order to provide a conservative estimate, the BRDF data from the Pathfinder sample CSIRO S/N 2 was used; which exhibits greater micro-roughness than the GO S/N 5 sample. The measured BRDF(θ) is described by the following analytic expression[1] for large angles. See “Scattering from coc surfaces” on page 2.

$$BRDF(\theta) = 2.53\times10^{-8}\cdot\theta^{-2.472}\,sr^{-1} \quad \text{for} \quad \theta > 3.4\times10^{-5}\,rad \quad .$$

The differential light power scattered from the COC into the solid angle subtended by the vacuum housing walls, scattered by the wall onto the surface of the COC, then rescattered from the COC back into the solid angle of the IFO beam is given by

$$dP_s = P_{ac}\cdot BRDF_{COC}\cdot d\Omega\cdot BRDF_{wall}\cdot\frac{A_{COC}}{l^2}\cdot BRDF_{COC}\cdot\Delta\Omega\,,$$

where P_{ac} is the arm cavity power incident on the COC, $d\Omega$ is the differential solid angle of the wall element, A_{COC} is the area of the COC, l is the distance to the scattering wall, and $\Delta\Omega$ is the

1. Scattered Light and its Control in the LIGO Beam Tubes, Albert Lazzarini, LIGO Science Meeting Talk, 4/1/97

LIGO-DRAFT

solid angle of the ITM beam.
$d\Omega = 2\pi \sin\theta d\theta = 2\pi\theta d\theta$;

and $\theta = \frac{r}{l}$ using a small angle approximation, where r is the radial distance from the COC mirror center to the scattering surface.

The mirror offset effect on the scattering angle will be approximated by separating the scattering geometry into two half-cylinders and averaging the sum of the contributions from each half-cylinder, as shown in figure 8. The radius of the negative mirror-offset half-cylinder is $r_{neg} = (r - r_0)$, and the radius of the positive mirror-offset half-cylinder is $r_{pos} = (r + r_0)$.

.

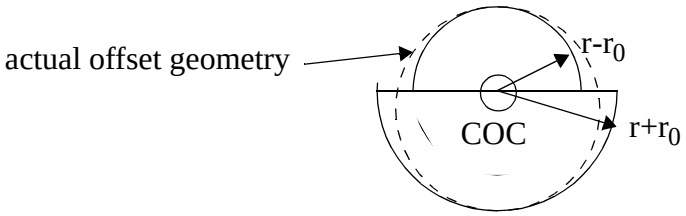

end view toward COC

Figure 8: Split geometry to approximate mirror offset effects

The total power scattered by a segment of wall which is subtended between the angles θ_1 and θ_2 is calculated by evaluating the integral.

$$P_s = P_{ac} \cdot A_{coc} \cdot BRDF_{wall} \cdot \Delta\Omega \cdot \frac{2\pi}{r^2} \cdot \int_{\theta_1}^{\theta_2} (2.53\times10^{-8} \cdot \theta^{-2.472})^2 \cdot \theta^3 d\theta$$

then

$$P_s = P_{ac} \cdot A_{coc} \cdot BRDF_{wall} \cdot \Delta\Omega \cdot \frac{2\pi}{r^2} \cdot \left(\frac{6.4\times10^{-16}}{0.944}\right) \cdot (\theta_1^{-0.944} - \theta_2^{-0.944})$$

The scattered power was calculated assuming the following values for the BRDF of the baffled beam tube and the unbaffled vacuum manifold walls, and the other parameters:

$BRDF_{beamtubebaffle} = 0.001 sr^{-1}$

$BRDF_{manifoldwall} = 0.1 sr^{-1}$

$\Delta\Omega = 2.7\times10^{-10} sr$

$A_{COC} = 4.9\times10^{-2} m^2$

$r = 0.91m, 0.62m$, for large and small manifold respectively.

LIGO-DRAFT

$r_0 = 375mm$

$P_{ac} = 10\times10^3 watt,$

3.2.4. Cryopump Surface Light Scattering

The cryopump surface inner lining, as shown in figure 9, can intercept scattered light from the ITM and ETM mirror surfaces at the near end of each beam tube, and the right-angle edge can retro-reflect back into the IFO. The retro-reflected cryopump light may exceed the LIGO

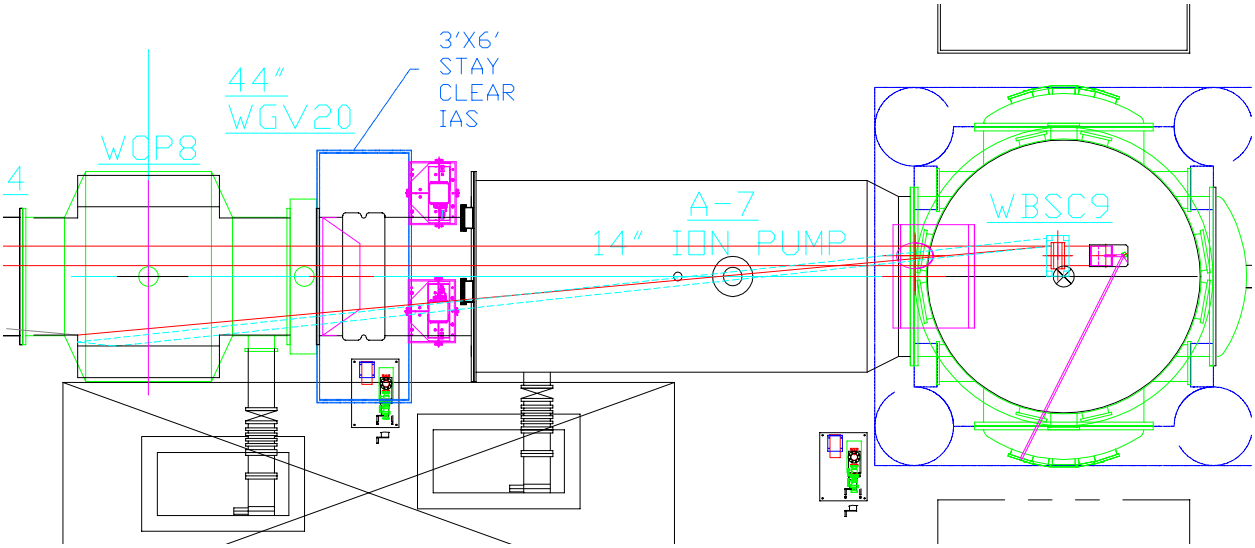

Figure 9: Retro-reflection from cryopump baffle

scattering requirements and *therefore baffles must be provided to hide the cryopump surfaces of CP2 and CP8 from the nearby COC. The far side of the cryopump does not need to be baffled,* because the 1.13m inside diameter of the cryopump surface is occluded from the far end of the beam tube by the 1.06m inside diameter of the beam tube baffles.

The cryopump lining may become coated with ice crystals or with areas of ice, so the BRDF of the surface is not predictable. However, a worst-case estimate of the scattering properties will be made by *assuming that the total integrated light which hits the inner surface of the cryopump will retro-reflect from the inside corner back to the COC which produced the incident light.* Then the COC will re-scatter the retro-reflected light into the IFO solid angle.

The differential power entering the IFO from this path can be calculated as follows,

$dP_r = P_{ac} \cdot BRDF_{COC} \cdot d\Omega \cdot BRDF_{COC} \cdot \Delta\Omega;$

and the total retroreflected power is obtained as before by integrating over the solid angle subtended by the cryopump surface.

$$P_r = P_{ac} \cdot \Delta\Omega \cdot 2\pi \cdot \left(\frac{6.4\times10^{-16}}{2.944}\right) \cdot (\theta_1{}^{-2.944} - \theta_2{}^{-2.944})$$

LIGO-DRAFT

The results of the calculation are presented in Summary of Beam-tube, Vacuum Manifold, and Cryopump Scattering Calculations on page 11.

3.2.5. Beam-tube Baffle Scattering

The large surface area of the beam tubes will cause excessive scattering of the diffuse light from the COC mirrors back into the IFO. This was recognized in the early design of LIGO, and baffles have been placed inside the beam tubes to block the diffuse light. The results of the calculations presented below indicate that a beam-tube baffle $BRDF_{beamtubebaffle} = 0.001 sr^{-1}$ is adequate to meet the enhanced LIGO requirement.

3.2.6. Summary of Beam-tube, Vacuum Manifold, and Cryopump Scattering Calculations

The results of the scattering calculations are presented in Table 2, “2K ITM Diffusely Scattered Power from Beam-tube and Vacuum Manifold Segments into IFO,” on page 11, and Table 3, “4K ETM Diffusely Scattered Power from Beam-tube and Vacuum Manifold Segments into IFO,” on page 12.
The scattered power from the 2K ITM should be interpreted as follows, referring to figure 6 and to the average scattered power column in Table 2 on page 11: the segment of wall from the mid station through the A-7A does not scatter; the 3m length of exposed wall included within the A-1C and the BE-4C scatters 2.7E-22 watts; the baffles in the beam tube scatter 3.0x10^{-21} watts;...etc.

Table 2: 2K ITM Diffusely Scattered Power from Beam-tube and Vacuum Manifold Segments into IFO

	r-r_0, mirror offset negative		*r+r_0, mirror offset positive*		*average offset*	
scattering distance from 2K ITM, m	*scattered power per length interval, watt*	*scattering angle, negative-mirror offset, rad*	*scattered power per length interval, watt*	*scattering angle, positive-mirror offset, rad*	*average scattered power, watt*	*description*
2000		1.220E-04		4.970E-04		mid station
1992	0.00E+00	1.225E-04	0.00E+00	4.991E-04	0.00E+00	3m length of 1.2 ID tubing (A-1C, BE-4C)
1989	4.30E-22	1.227E-04	1.14E-22	4.997E-04	2.72E-22	end 2000m beam tube
37	4.77E-21	4.235E-03	1.28E-21	2.473E-02	3.03E-21	begin 2000m beam tube
37	0.00E+00	6.667E-03	0.00E+00	2.716E-02	0.00E+00	end 1.2 ID tube
35	4.31E-22	7.052E-03	1.15E-22	2.873E-02	2.73E-22	2m length 1.2 ID tubing (BE-4A)

SO-DRAFT

30	0.00E+00	8.106E-03	0.00E+00	3.302E-02	0.00E+00	end of CP2
28	4.84E-16	8.683E-03	7.75E-18	3.537E-02	2.46E-16	begin CP2
28	0.00E+00	8.683E-03	0.00E+00	3.537E-02	0.00E+00	end transition tube
7.6	2.57E-21	7.099E-02	6.11E-22	1.697E-01	1.59E-21	1.8 ID transition tube (B-9A, BE-5A, B-1a, B-8A)
		total			**2.46E-16**	
		initial LIGO requirement[a]			**1.50E-17**	
		enhanced LIGO requirement[b]			**1.50E-21**	

a. See the requirement for diffuse scattered light from ETM and ITM, Table 1 on page 11.
b. The enhanced LIGO requirement for strain amplitude density is a factor 1E-2 lower than the initial LIGO requirement (Ref. SRD, LIGO-E950018-02-E); so the strain power density requirement is a factor 1E-4 lower. Therefore the enhanced LIGO noise power requirement will also be a factor 1E-4 lower.

As shown in the table, the unbaffled cryopump surfaces of CP2 may retro-reflect 2.5×10^{-16} watts; which exceeds the initial LIGO requirement.

Therefore a CP2 baffle is needed.

The scattered power from the 4K ITM should be interpreted in a similar manner, referring to figure 7 and to the average scattered power column in Table 3 on page 12: the 5m length of exposed wall included within the A-14A and the BE-4E scatters $4.9\text{x}10^{-22}$ watts; the baffles in the beam tube scatter $3.1\text{x}10^{-21}$; etc. As shown in the table, the unbaffled cryopump surfaces of CP8 may retroflect 1.6×10^{-17} watts, which barely meets the initial LIGO requirement. *Therefore a CP8 baffle is needed.*

Table 3: 4K ETM Diffusely Scattered Power from Beam-tube and Vacuum Manifold Segments into IFO

	r-r$_0$, mirror offset negative		*r+r$_0$, mirror offset positive*		*average offset*	
scattering distance from 4K ETM, m	*scattered power per length interval, watt*	*scattering angle, negative-mirror offset, rad*	*scattered power per length interval, watt*	*scattering angle, positive-mirror offset, rad*	*average scattered power, watt*	*description of scattering location*
2000		1.220E-04		4.970E-04		mid station
1992	0.00E+00	1.225E-04	0.00E+00	4.991E-04	0.00E+00	5m length of 1.2 tubing (A-14A, BE-4E)
1987	7.75E-22	1.228E-04	2.06E-22	5.003E-04	4.90E-22	end 2000m beam tube
11.5	4.88E-21	1.348E-02	1.30E-21	7.870E-02	3.09E-21	begin 2000m beam tube

LIGO DRAFT

11.5	0.00E+00	2.122E-02	0.00E+00	8.643E-02	0.00E+00	end 1.0 tube
10.0	3.46E-22	2.440E-02	9.19E-23	9.940E-02	2.19E-22	end CP8
8.8	3.23E-17	2.773E-02	5.18E-19	1.130E-01	1.64E-17	begin CP8
7.3	3.52E-22	3.342E-02	9.34E-23	1.362E-01	2.22E-22	1.5m length 1.0 tubing (A-1E)
7.3	0.00E+00	3.342E-02	0.00E+00	1.362E-01	0.00E+00	end transition tube
5.0	5.59E-22	1.079E-01	1.00E-22	2.579E-01	3.30E-22	1.8 ID transition tube (A-7C)
		total			**1.64E-17**	
		initial LIGO requirement[a]			**1.50E-17**	
		enhanced LIGO requirement[b]			**1.50E-21**	

a. See the requirement for diffuse scattered light from ETM and ITM, Table 1 on page 11.
b. The enhanced LIGO requirement for strain amplitude density is a factor 1E-2 lower than the initial LIGO requirement (Ref. SRD, LIGO-E950018-02-E); so the strain power density requirement is a factor 1E-4 lower. Therefore the enhanced LIGO noise power requirement will also be a factor 1E-4 lower.

3.3. COC Elliptical Baffles for Recycling Cavity

A portion of the main beam in the recycling cavity will spill over the periphery of the 250 mm diameter BS, which is tipped at 45 deg to the beam axis. The main beam is displaced by 7.8 mm as it passes through the BS. The input beam will be shifted by half this amount so that the displacement is shared on both sides, then the BS presents an elliptical cross-section to the main beam with a semi-major axis of 125 mm and a semi-minor axis of 80.6 mm.

The fraction of the total power which hits the BS mirror is calculated by integrating the normalized intensity of the Gaussian profile laser beam across the elliptical cross-section of the mirror.

$$I(x,y) := \frac{2 \cdot e^{-2 \cdot \left(\frac{x^2 + y^2}{w^2} \right)}}{\pi \cdot w^2}$$

$$f_M := \frac{2}{\pi \cdot w^2} \int_{-a}^{a} \int_{0}^{b \cdot \sqrt{1 - \frac{x^2}{a^2}}} 2 \cdot e^{-2 \cdot \frac{y^2}{w^2}} dy \cdot e^{-2 \cdot \frac{x^2}{w^2}} dx$$

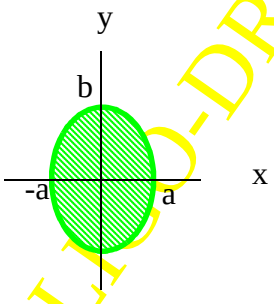

LIGO-DRAFT

where a is the semi-minor axis, and b is the semi-major axis of the elliptical cross-section.

3.3.1. Glint Power into the IFO from the Light Spilling Around the BS Mirror

A fraction of the power that spills over the sides of the BS may hit the walls of the vacuum enclosure and cause a glint back into the IFO.

$$P_g = P_{ann} \cdot \frac{2R\lambda}{\pi^2 w^2} \eta_{glint}.$$

3.3.2. Power Scattered from the Elliptical Baffle into IFO

The power spilling over the BS mirror will be blocked with an isolated elliptical baffle mounted to the LOS structure. However, the baffle itself will scatter a lesser amount of power into the IFO.

$$P_s = P_{BS} \cdot BRDF \cdot \Delta\Omega \cdot A_{SEI},$$

where the scattered power has been effectively reduced by the seismic attenuation factor, A_{SEI}.

The elliptical baffle also causes edge diffraction into the IFO, but the seismic isolation factor reduces the effective diffracted light to a safe level, as shown in Table 4 on page 14. See “Edge Diffraction from COC Baffle Aperture” on page 30.

3.3.3. Summary of Elliptical Baffle Calculations

The summary of the glint and scattered power in Table 4 on page 14 indicates that the light power spilling around the BS *must be caught with seismically isolated baffles,* in order to meet the glint criterion.

Table 4: Summary of Light Spilling Around BS

Parameter	*4K*	*2K*
power in the recycling cavity, watt	300	300
beam parameter, w, mm	36.4	32.0
BRDF of elliptical baffle, sr^{-1}	0.01	0.01
IFO solid angle, sr	2.7×10^{-10}	2.7×10^{-10}
seismic isolation factor	3.6×10^{-9}	3.6×10^{-9}
semi-major axis, b, mm	125	125
semi-minor axis, a, mm	80.6	80.6
fractional power spilled around BS, watt	1.26×10^{-5}	6.3×10^{-7}

LIGO-DRAFT

Table 4: Summary of Light Spilling Around BS

Parameter	*4K*	*2K*
power spilling toward RM, watt	1.89×10^{-3}	9.4×10^{-5}
power spilling toward ITMx, watt	3.78×10^{-3}	1.9×10^{-4}
power spilling toward AP, watt	1.89×10^{-3}	9.4×10^{-5}
glint power, RM beam, watt	4.6×10^{-12}	3.0×10^{-13}
glint power, ITMx beam, watt	9.2×10^{-12}	6.0×10^{-13}
glint power, AP beam, watt	4.6×10^{-12}	3.0×10^{-13}
total glint power, all beams, watt	1.8×10^{-11}	1.2×10^{-12}
total scattered power from wall, watt	1.9×10^{-14}	4.4×10^{-18}
total scattered power from isolated elliptical baffles, watt	7.4×10^{-23}	3.6×10^{-24}
edge diffraction from isolated elliptical baffle, watt	3.1×10^{-31}	4.7×10^{-34}
scattered light requirement per path, watt	3.3×10^{-13}	3.3×10^{-13}

Elliptical baffles which match the apparent elliptical cross-section of the 45 degree BS will be placed in front of the RM, ITMx, and ITMy, as shown in figure 10; so that the glint does not exceed the scattering requirements.

LIGO-DRAFT

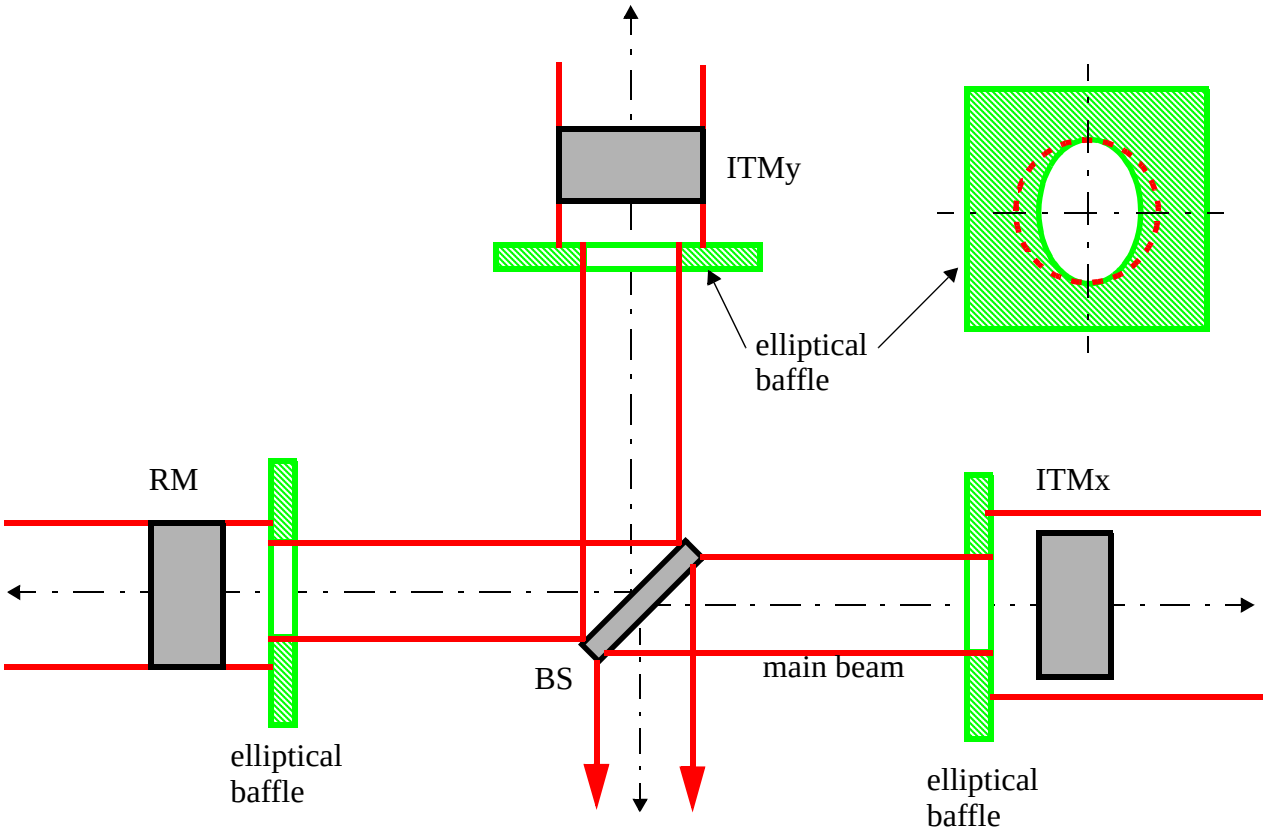

Figure 10: Elliptical baffles for RM, ITMx, and ITMy

3.4. Are Baffles Needed for the PO Mirrors?

The BS, ITM, and ETM pick-off mirror apertures are smaller than the raw pick-off beams coming from the COC mirrors, as shown in figure 11. The spill-over power may cause a glint from the vacuum housing walls behind the PO mirror. The glint power without the baffle, the edge diffraction, and the scattered power from the PO mirror baffles were calculated as before. The results are presented in Table 5 on page 17, and in Table 6 on page 18.
PO mirror baffles are not needed.

LIGO-DRAFT

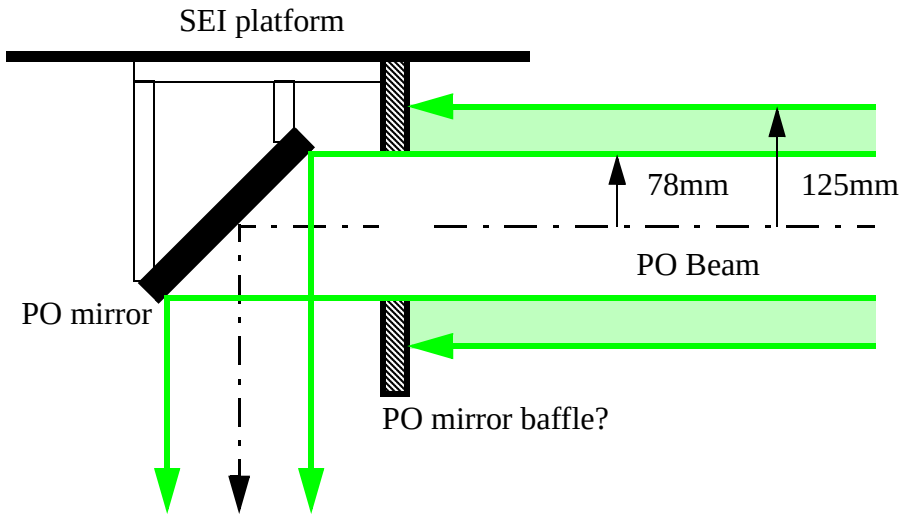

Figure 11: Baffle for PO Mirrors are not needed

Table 5: Summary of 4K PO Mirror Baffle Calculations

	ITM	*ETM*	*BS*
baffle $BRDF_{baff}$, sr^{-1}	1×10^{-2}	1×10^{-2}	NA
baffle transmissivity, maximum	7.4×10^{-1}	1.4×10^{-2}	NA
beam parameter, w, mm	36.3	45.7	36.3
baffle aperture radius, mm	78	78	78
PO beam power, watt	0.14	0.39	0.075
power spilling around PO mirror aperture, watt	1.4×10^{-5}	1.2×10^{-3}	7.3×10^{-6}
glint power into IFO beam without baffle, watt	1.2×10^{-20}	1.3×10^{-20}	1.7×10^{-20}
scattered light requirement per path, watt	6.8×10^{-16}	3.2×10^{-18}	6.8×10^{-16}

LIGO-LHT

Table 6: Summary of 2K PO Mirror Baffle Calculations

	ITM	*ETM*	*BS*
baffle $BRDF_{baff}$, sr^{-1}	NA	1×10^{-2}	NA
baffle transmissivity, maximum	NA	8.5×10^{-2}	NA
beam parameter, w, mm	26.9	31.5	26.9
baffle aperture radius, mm	78	78	78
PO beam power, watt	0.14	0.39	0.075
power spilling around PO mirror aperture, watt	7.0×10^{-9}	1.8×10^{-6}	3.7×10^{-9}
glint power into IFO beam without baffle, watt	1.2×10^{-23}	4.4×10^{-23}	1.5×10^{-24}
scattered light requirement per path, watt	6.8×10^{-16}	3.2×10^{-18}	6.8×10^{-16}

Baffles are not needed for the PO mirrors because the glint power does not exceed the scattering requirements.

3.5. Mode-cleaner Baffles

The scattered light from the mode-cleaner mirrors will eventually spill around each of the mirrors in the form of an annular beam. These three annular beams may hit a chamber wall and cause a glint or scatter into the IFO beam. The annular beams around mirrors MC1 and MC2 will be caught at the source by mounting baffles to the outside of the SOS structures which support the mode-cleaner mirrors. The baffle at MC1 will provide an aperture for passage of the primary laser beam, as shown in figure 12. Part of the annular beam around MC3 will pass through the mode matching telescope and be caught by the COC baffle in front of the RM.

The requirement for the light amplitude scattered back into the mode-cleaner will be taken to be 100 times greater than the scattered light amplitude allowed in the IFO. Then the scattered power requirement for light from the mode-cleaner entering through the RM is 10000x 5.8×10^{-13}, $P_s)_{REQmodecleaner} = 5.8\times10^{-9}$.

Baffles will be mounted on the SOS structure to catch the scattered light from the mode-cleaner mirrors, even though the glint does not exceed the scattered light requirement; because of the inordinately large amount of power scattered from the mode-cleaner.

A summary of the scattered light calculations for the mode-cleaner is presented in Table 7 on page 19.

LIGO-DRAFT

Table 7: Summary of Light Spilling Around Mode-cleaner Mirrors

Parameter	*4K*	*2K*
power in the mode-cleaner cavity, watt	9300	9300
beam parameter, w, mm	2.0	2.0
BRDF of elliptical baffle, sr^{-1}	0.01	0.01
elliptical baffle transmissivity, maximum	2.8×10^{-4}	2.8×10^{-4}
IFO solid angle, sr	2.7×10^{-10}	2.7×10^{-10}
seismic isolation factor	3.6×10^{-9}	3.6×10^{-9}
power spilling around mode-cleaner mirrors, watt	0.27	0.27
glint power back into mode-cleaner, watt	8.0×10^{-11}	8.0×10^{-11}
total scattered power from wall, watt	7.3×10^{-13}	7.3×10^{-13}
total scattered power from isolated baffles, watt	2.6×10^{-21}	2.6×10^{-21}
scattered light requirement, watt	5.8×10^{-9}	5.8×10^{-9}

LIGO-DRAFT

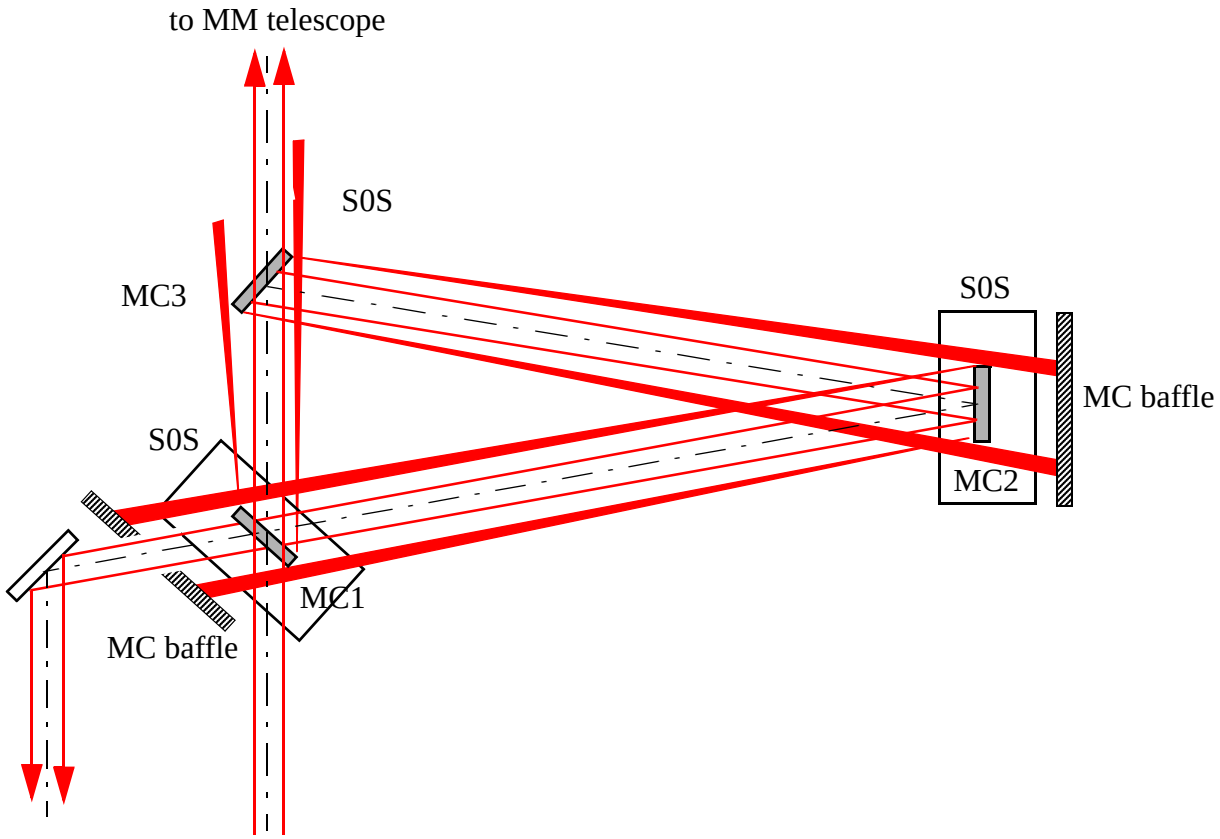

Figure 12: Mode-cleaner baffles, mounted to SOS structure

APPENDIX 1

4 GHOST BEAM GLINT CALCULATIONS

Those ghost beams that are not dumped may hit a surface and cause a glint back into the IFO. The worst case glint from a chamber wall will occur when the ghost beam hits a cylindrical surface aligned exactly perpendicular to the ghost beam direction, as shown in the figure 13 (note: the surface can be either convex or concave). An example of such a glint surface might be the inner wall of the BSC housing.

The ghost beam glint from the reflecting surface will retroreflect into the solid angle of the IFO, provided the tilt of the curved surface is within the diffraction angle of the IFO beam. The maximum illuminated area of the glint surface which meets these conditions is

$$A_g = R\theta_d w = R \cdot \left(\frac{2}{\pi} \cdot \frac{\lambda}{w}\right) \cdot w = \frac{2}{\pi} R\lambda .$$

LIGO-DRAFT

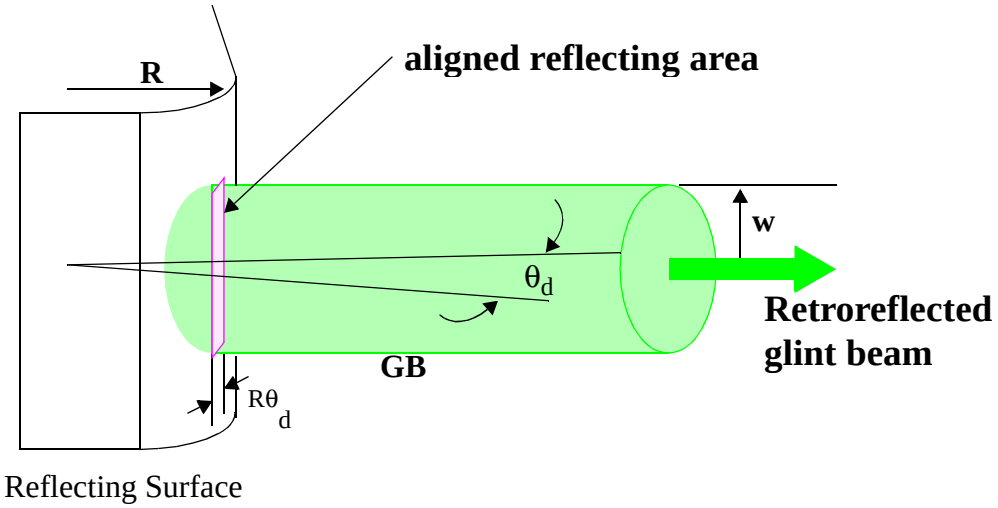

Figure 13: Glint Reflection of $GBAR_3$ Back Into the IFO

The retroreflected light from the glint into the IFO is proportional to the incident power, to the ratio of glint area to ghost beam area, and to the return transmissivity through the COC. An additional factor, the glint efficiency η_{glint}, has been included to account for the roughness of the surface and the coherent reduction of the reflected amplitude due to interference effects. See "Glint Efficiency" on page 21.

$$P_g = P_i \cdot \frac{2R\lambda}{\pi^2 w^2} \cdot T\eta_{glint}.$$

The width of the glint surface is $l = \frac{2}{\pi} \cdot \frac{R\lambda}{w}$. The geometric optics approximation is valid for $l \gg \lambda$; so with a 1.064 micron wavelength beam, the approximation is valid for $R > 0.4m$

We will estimate the glint power assuming a radius of R=1.5m, which corresponds to the inside wall of the BSC chamber, using the following parameters:

R=1.5m
w=0.0364 m

$\theta_d = 9.3\times10^{-6}$ rad,

$\eta_{glint} = 1\times10^{-5}$

$P_g = 2.43\times10^{-9} P_i T$

4.1. Glint Efficiency

Two different phenomena associated with the surface roughness account for a reduction in the glint power; 1) the random surface curvature causes a local deviation of the reflected beam power away from the IFO solid angle, and 2) the optical path length differences due to local surface

LIGO-DRAFT

irregularities causes a reduction in the reflected wave amplitude because of coherent wave interference across local regions of the surface.

4.1.1. Surface Curvature Efficiency

The glint area consists of a narrow strip a few tens of wavelengths wide with a length equal to the beam diameter. Along the length of the glint strip the surface topology will change drastically due to the surface irregularity and surface roughness. It will be assumed that the surface height does not change across the width because the dimension is so small, and that the surface variation can be treated as a one-dimensional function. The topology of the glint surface is shown schematically in figure 14

.

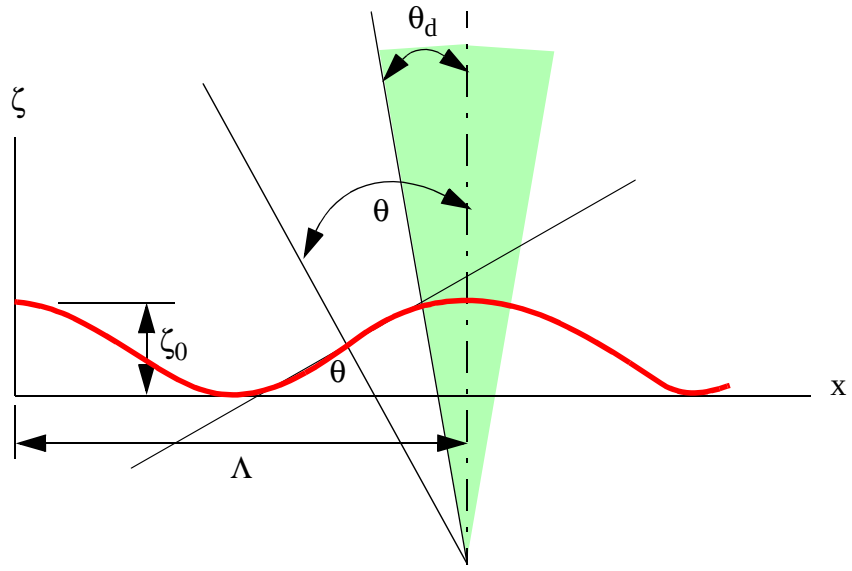

Figure 14: Topology of the glint surface

Only the local surfaces that are tilted within the diffraction angle of the IFO beam will reflect light power into the beam, so the surface curvature efficiency can be defined as the fraction of surface angles which are less than the IFO diffraction angle.

For the purpose of estimating the local surface curvatures, we will assume that the surface amplitude spectrum can be described as a spatial frequency power law

$\zeta_{0\nu} = A_0 \nu^{-n}$, where the amplitude coefficient is related to the maximum surface height at the lowest frequency by

$A_0 = \zeta_0 \nu_0^n$.

The spatial frequency is related to the period of the surface ripple component

$$\nu = \frac{2\pi}{\Lambda}.$$

A typical component of the surface spectrum can be described mathematically as

LIGO-DRAFT

$\zeta = \zeta_{0\nu}\cos\left(\frac{2\pi}{\Lambda}\right)$.

The local tilt of the surface is given by

$\theta = \frac{d\zeta}{dx} = -\zeta_{0\nu}\frac{2\pi}{\Lambda}\sin\left(\frac{2\pi x}{\Lambda}\right)$, and the condition for a glint reflection is $|\theta| \le \theta_0$.

This places a limit on the maximum fractional length within a component surface period which can contribute to the glint,

$$\frac{x_m}{\Lambda} \le \frac{1}{2\pi}\sin\left(\theta_0\frac{\Lambda}{2\pi\zeta_{0\nu}}\right)^{-1}$$

The total fractional contribution, which will be defined as the glint surface efficiency, is obtained by integrating over all possible surface ripple components, from the minimum to the maximum spatial frequencies.

$$\eta_{\text{glint\_sur}}(\nu_m) := \int_{\nu_0}^{\nu_m} \frac{\operatorname{asin}\left(\frac{\theta_0}{\nu\cdot\zeta_{0\nu}(\nu)}\right)}{2\cdot\pi\cdot(\nu_m-\nu_0)}\,d\nu$$

This expression was evaluated assuming a $1/\nu$ surface spectral distribution law, with the following parameters.

IFO divergence angle	$\theta_0 = 9.3\times10^{-6}$ rad
minimum spatial frequency	$\nu_0 = 0.17$ 1/mm
maximum surface height	$\zeta_0 = 0.2$ mm

Then $\eta_{glintsur}(\nu_m) = 4.3\times10^{-5}$,

and the value is independent of the maximum surface frequency because of the assumed $1/\nu$ surface spectral distribution law.

4.1.2. Coherence Efficiency

The beam illuminating the glint area is coherent across the entire length of the area and the entire area is within a resolution element of the COC mirror, therefore the net reflected light amplitude is the algebraic sum of the differential reflected amplitudes with varying phases across the length of the glint surface.

The differential reflected light wave amplitude due to a particular spatial frequency component is $dE = E_0\cos\left(\frac{4\pi}{\lambda}\zeta_{0\nu}(\nu)\right)$, and the total amplitude is obtained by integrating over all possible spatial frequencies. The square of the ratio of net amplitude to peak amplitude will be defined as the

LIGO-DRAFT

glint coherence efficiency.

$$\eta_{glint\_coh}(\nu_m) := \left[\int_{\nu_0+\delta}^{\nu_m} \frac{\cos\left(4 \cdot \frac{\pi \cdot \zeta_{0\nu}(\nu)}{\lambda}\right)}{(\nu_m - \nu_0 - \delta)} d\nu \right]^2$$

4.1.3. Total Glint Efficiency

The total glint power efficiency is the product of the two efficiencies. The results are plotted in figure 15.

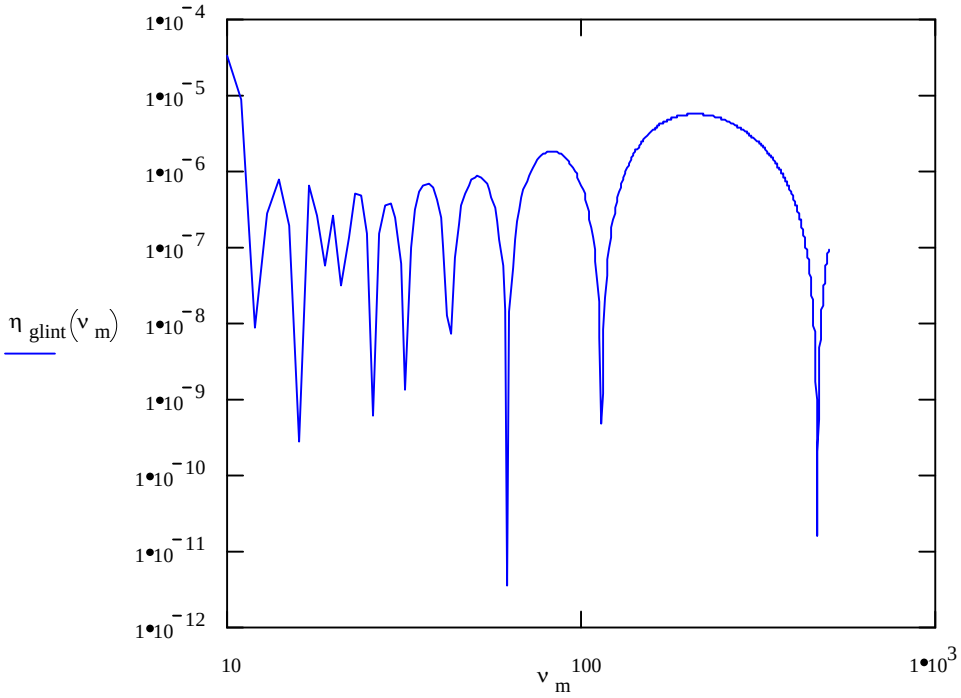

Figure 15: Total glint efficiency as a function of maximum spatial frequency

From figure 15, we can estimate the maximum glint efficiency, $\eta_{glintmax} < 1 \times 10^{-5}$.

APPENDIX 2

5 EDGE DIFFRACTION

Edge diffraction occurs whenever a coherent wavefront is terminated abruptly at a boundary such as the edge of a mirror, the edge of a baffle, or the edges of an aperture in a baffle. The magnitude

LIGO-DRAFT

of the power diffracted back in the direction of the incident beam, within the acceptance solid angle of the IFO, can be estimated using the Sommerfeld solution for diffraction from a semi-infinite plane with approximations to the Fresnel integral. The simplified geometry of the problem is shown in figure 16 below.

The diffracted field amplitude a long distance away from the edge, $kr \gg 1$, is given approximately by

$$E_d = u_0 \cdot \frac{\sin\frac{\alpha_0}{2} \cdot \sin\frac{\theta}{2}}{\cos\theta + \cos\alpha_0} \cdot \frac{1}{\sqrt{kr}}$$

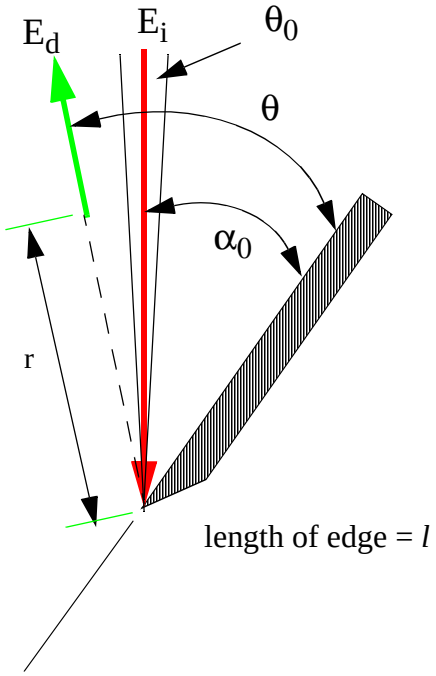

Figure 16: Edge diffraction geometry

The diffracted field has a peak value approximately equal to the incident field along the specular direction, i.e.

$E_d = \frac{u_0}{\sqrt{kr}} = E_i$, for $\theta = \pi - \alpha_0$; so we can evaluate the diffracted field source term at a sufficiently close distance to the edge where the approximation is still valid, e.g. $r = 10\lambda$, then $u_0 = \sqrt{10k\lambda}$, and

$$E_d = E_i \cdot \sqrt{10\frac{\lambda}{r}} \cdot \frac{\sin\frac{\alpha_0}{2} \cdot \sin\frac{\theta}{2}}{\cos\theta + \cos\alpha_0}.$$

The total power diffracted into the solid angle of the IFO beam is given by

LIGO-DRAFT

$P_d = \int E_d^2 dA$,

where the area element is the differential surface element of a cylinder with height equal to the diffracting edge of length *l*, then

$dA = r d\theta l$.

The integral must be evaluated within the acceptance angle of the IFO, where $\theta_0 = 9.3\times10^{-6}$ rad is the divergence half-angle of the IFO beam.

$$P_d = \int_{\alpha_0 - \theta_0}^{\alpha_0 + \theta_0} E_i^2 \cdot 10\frac{\lambda}{r} \cdot \left(\frac{\sin\frac{\alpha_0}{2} \cdot \sin\frac{\theta}{2}}{\cos\theta + \cos\alpha_0} \right)^2 \cdot r l d\theta .$$

For typical small values, i.e. $\theta_0 \ll \alpha_0$,

$$P_d = E_i^2 \cdot 10\lambda l \cdot \frac{\sin\frac{\alpha_0}{2}^4}{4\cos\alpha_0^{\,2}} \cdot 2\theta_0 .$$

The field amplitude can be evaluated from the total integrated power in the Gaussian beam which is incident on the edge.

$$E_i^{\,2} = \frac{P_T}{\pi w^2/2} \cdot e^{-2r_0^2/w^2},$$

where P_T is the total power in the beam. Then the diffracted power can be written as

$$P_d = \frac{P_T}{\pi w^2/2} \cdot e^{-2r_0^2/w^2} \cdot 10\lambda l \cdot \frac{\sin\frac{\alpha_0}{2}^4}{4\cos\alpha_0^{\,2}} \cdot 2\theta_0$$

Aside from the trigonometric factor, the result can be interpreted as a cylindrical wave diffracting from a line source of length *l* and width 10λ into the solid angle of the IFO.

5.1. Effective Edge Length Reduction Due to Coherence Effects

The baffle aperture edge is inclined with respect to the incident beam direction, as shown in figure 17, and the phase of the diffracted light wave varies along the edge due to the optical path differences. The edge-diffracted light within a coherence length will overlap on the COC and will add coherently in amplitude. The resultant amplitude within each coherence region is the algebraic sum of the differential amplitudes along the edge path. Most of the edge will produce a negligible contribution to the net wave amplitude because the optical phase changes rapidly over many cycles, and the principal amplitude contribution will come from small edge segments at the top and bottom of the aperture. Diffracted light from adjacent coherence regions will not overlap on the COC, and the total diffracted power is the sum of the diffracted power from each coherence region.

We will assume that each portion of the edge has a constant phase relationship with respect to the center of the aperture, even though the entire baffle may be vibrating. The coherence length is

LIGO DRAFT

essentially the diameter of the resolved spot at the baffle location as seen from the COC at the far end of the beam tube, which is about the size of the Gaussian beam parameter w of the main IFO beam.

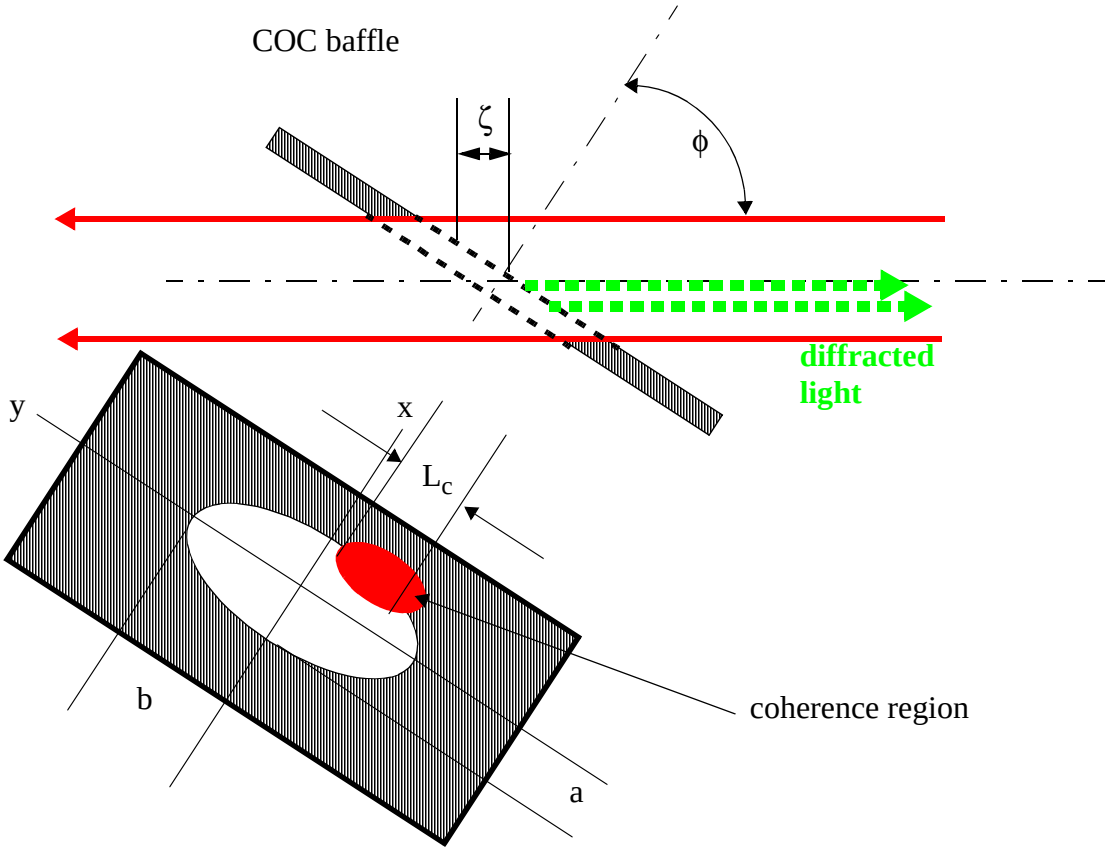

Figure 17: Coherence region on aperture edge

The total edge-diffracted power into the IFO is given by

$P = K\sum_j \langle E_j \rangle^2 l\lambda$, where K is the Sommerfeld geometric function and l is the length of the aperture edge. The field strength will be expressed in terms of the peak field amplitude along the edge multiplied by an edge efficiency, which will be derived below.

$P = KE_0^2 \eta_{edge} l\lambda$

The optical path difference at a position y along the edge is

$\Delta\zeta = 2y\sin\phi$, where ϕ is the tilt angle of the baffle. The net light amplitude within the jth coherence region is the sum of the differential amplitudes along the edge

LIGO-DRAFT

$E_j = \frac{E_0}{S}\int_{y_j}^{y_{j+1}} \cos\left(\frac{4\pi y \sin\phi}{\lambda}\right) ds$, where the differential path along the edge can be expressed in terms of the y coordinate

$$ds := \frac{dy}{\sin\left[\operatorname{atan}\left[-\sqrt{\left(\frac{b(\phi)^4}{a^2 \cdot y} - \frac{b(\phi)^2}{a^2}\right)}\right]\right]}$$

The semi-major axis of the elliptical aperture, b, is taken along the y-axis. The semi-minor axis, a, is taken along the x-axis. The arc length along the aperture edge measured from y=0 is given by the path integral.

$$s(y) := \int_0^y \frac{1}{\sin\left[\operatorname{atan}\left[-\sqrt{\left(\frac{b(\phi)^4}{a^2 \cdot u^2} - \frac{b(\phi)^2}{a^2}\right)}\right]\right]} du$$

For tilt angles > 5 deg, there are many wavelengths of optical path length change along the edge within the coherence region which will give a zero contribution, and only a small edge segment within each coherence region gives a non-zero contribution to the diffracted power. In fact, the principal contribution comes from the two edge segments at the top and bottom of the aperture.

A typical size of the coherence length is taken to be the Gaussian beam parameter projected onto the tipped baffle.

$$L_c(\phi) := \frac{w}{\cos(\phi)}$$

And there are

$$N(\phi) := \operatorname{ceil}\left(\frac{b(\phi)}{L_c(\phi)}\right)$$

coherence lengths within an aperture quadrant (the “ceil” function calculates the largest integer value).
The number of integral wavelengths within an optical path length is given by (the “floor” function calculates the smallest integer value)

$$N_\lambda(\phi, N) := \operatorname{floor}\left(\frac{\Delta\zeta(\phi, N)}{\lambda}\right)$$

The non-zero contributing edge length within the coherence region is

$$\Delta L(\phi, N) := \frac{\left(\Delta\zeta(\phi, N) - \lambda \cdot N_\lambda(\phi, N)\right)}{2 \cdot \sin(\phi)}$$

LIGO-DRAFT

The fraction of the edge in the jth region which produces edge diffraction is

$$\eta_{edgej}(\phi, N) := \left[\int_{yj(\phi, N) - \Delta L(\phi, N)}^{yj(\phi, N)} \frac{1}{s(\phi)} \cdot \cos\left(4 \cdot \pi \cdot y \cdot \frac{\sin(\phi)}{\lambda}\right) \cdot \frac{1}{\sin\left[\operatorname{atan}\left[-\sqrt{\left(\frac{b(\phi)^4}{a^2 \cdot y^2} - \frac{b(\phi)^2}{a^2}\right)}\right]\right]} dy \right]^2$$

and the total edge efficiency is the sum of the j regions

$$\eta_{edge}(\phi, N) := \eta_{edge1}(\phi, N) + \eta_{edge2}(\phi, N) + \eta_{edge3}(\phi, N) + \eta_{edge4}(\phi, N)$$

The edge efficiency is plotted in figure 18 as a function of tilt angle of the baffle aperture in radians, for N=4 coherence regions within the aperture quadrant. The maximum edge efficiency is described reasonably well by the expression, $\eta_{edgemax} = \frac{1 \times 10^{-6}}{\phi}$, as shown in figure 18.

.

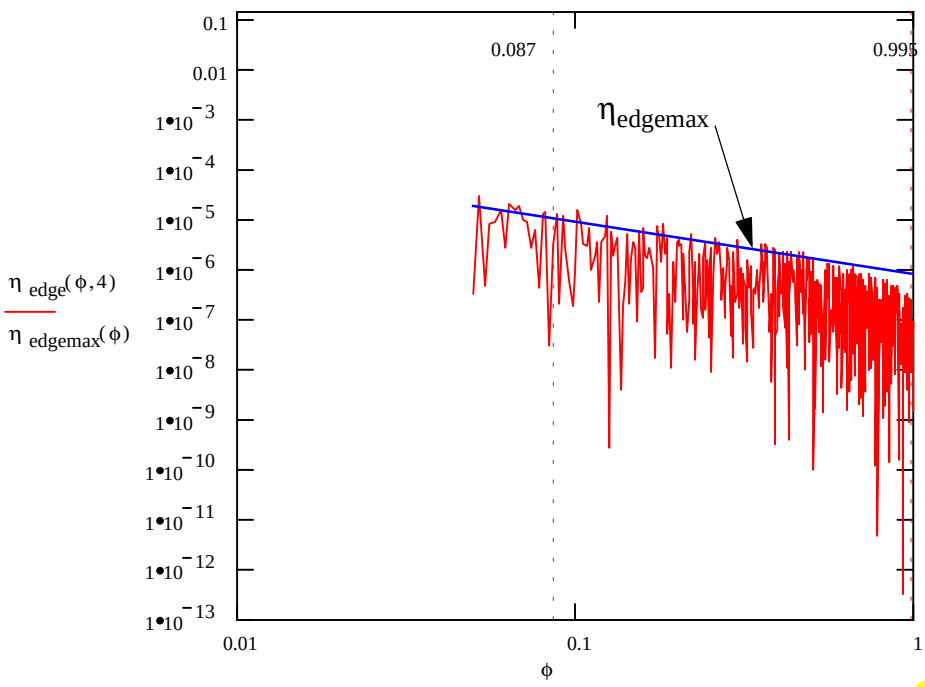

Figure 18: Edge diffraction efficiency, with N=4, as a function of baffle tilt angle

From the figure we can estimate that the edge diffraction efficiency for a 5 degree tilted baffle is $< 1 \times 10^{-5}$, and for a 57 degree tilted baffle is $< 1 \times 10^{-6}$.

LIGO-DRAFT

5.2. Edge Diffraction from COC Baffle Aperture

The edge diffraction of the main arm cavity beam from the aperture of the COC baffles can be calculated using the formalism developed above.

The Gaussian beam waist, w_0=35.1 mm, is located 975000 mm from the 4K ITM mirror. The distance to the 4K ETM mirror is 3025000 mm. The Gaussian beam parameter in millimeters at the ITM and ETM mirrors can be calculated using the Gaussian beam expansion formula.

$$w_{4KITM} := w_0 \cdot \left[1 + \left(\frac{\lambda \cdot z_{ITM}}{\pi \cdot w_0^2} \right)^2 \right]^{0.5}$$

Then w_{4KITM} 36.3 mm

w_{4KETM} 45.6 mm

The edge-diffracted power of a 5000 watt beam into the IFO from the ITM COC baffle with a 124 mm radius aperture as a function of complimentary incidence angle of the baffle surface, is shown in figure 19.

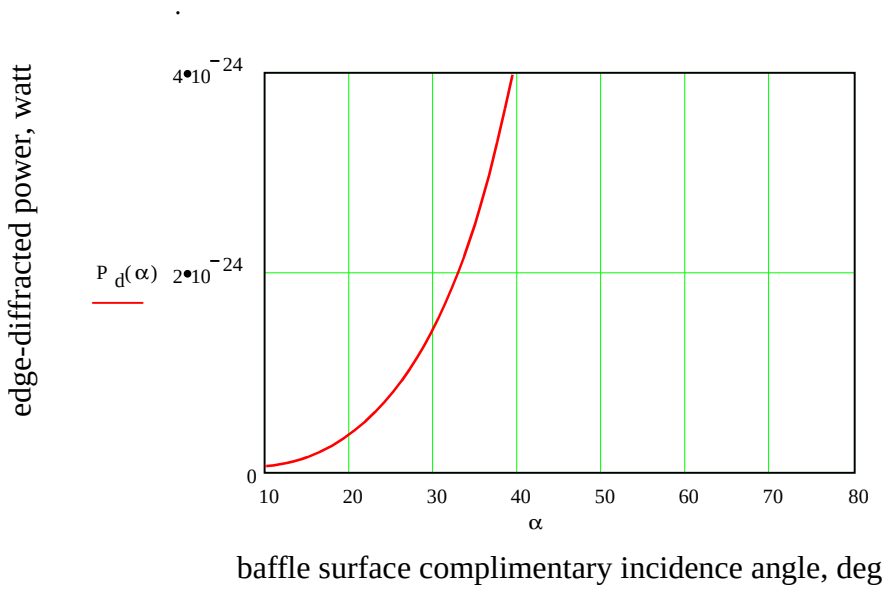

Figure 19: Edge-diffracted power into IFO from 5000 watt beam passing through 248 mm diameter aperture in the tilted ITM COC baffle

From figure 19 we can determine that the diffracted power into the IFO is 2.0×10^{-24} watts from the ITM COC baffle tilted 33 deg from the beam axis. Similarly, the power diffracted into the IFO from the ETM COC baffle with a 124 mm radius aperture was calculated to be 6.4×10^{-21} watts.

LIGO-DRAFT